

Design of a Low-Profile Antenna by Using Orthogonal Parasitic Meandered Monopoles

Mirko Barbuto^{1, *}, Fabrizio Trotta², Filiberto Bilotti³, and Alessandro Toscano³

Abstract—In this paper, we present the design of a low-profile antenna consisting of two orthogonal parasitic meandered monopoles excited by the near-field coupling with a feeding bow-tie. The two parasitic radiators and the driven element are placed on two different faces of the same dielectric substrate and a coaxial probe excites the bow-tie through a metallic ground plane. In this way, the antenna has compact dimensions of $21 \times 10.5 \times 1.6 \text{ mm}^3$ ($\lambda_0/6 \times \lambda_0/12 \times \lambda_0/75$, excluding the ground plane) and exhibits a good impedance matching in the 2.4–2.485 GHz Wi-Fi band with an overall efficiency around 50%.

1. INTRODUCTION

Monopole antennas have been widely used in mobile communication systems due to their simple structure, omnidirectional radiation pattern and size reduction compared to the equivalent dipole antennas. However, the length of a quarter-wave monopole ($\lambda_0/4$, where λ_0 is the free-space wavelength at the operating frequency) is often too long for modern communication systems, which are characterized by ever smaller available space for the radiating element. For this reason, several effective ways to reduce the antenna dimensions have been proposed, such as the use of fractal or meandered structures [1–3], shorting pins [4] and metamaterial-inspired resonators [5]. However, as it is evident by considering the fundamental limitations of electrically small antennas [6–8], bandwidth decreases when the antenna size decreases. Therefore, it is often difficult to simultaneously satisfy the requirements in terms of impedance bandwidth and overall dimensions.

In this work, in order to design a compact antenna with a good impedance matching in the 2.4 GHz Wi-Fi band, we propose to use two orthogonal meandered printed monopoles with slightly different dimensions. In this way, we are able to merge the two independent resonances of the monopoles to achieve a wideband response.

However, although the meandered structure can be seen as the simplest solution to reduce the monopole size, it can lead to difficulties in the impedance matching to the source. In order to overcome this issue, here we propose to use a metamaterial-inspired solution. In fact, metamaterial concepts have been widely used to design several radiating structures (see, for instance, [9–19]). Some of them [9, 14–17] are based on the employment of driven and parasitic elements that allow obtaining nearly complete impedance matching to the source and high radiation efficiency. Following this approach, although the two monopoles are the main radiating elements, in our case they are not connected to the feeding coaxial cable, but act as parasitic resonators of a feeding bow-tie. The proposed structure can be thus considered as a new element of the novel class of metamaterial-inspired near-field resonant parasitic antennas [14, 15], which are based on the use of radiating parasitic resonators excited by the near-field coupling with a feeding structure.

Received 19 June 2015, Accepted 31 July 2015, Scheduled 15 August 2015

* Corresponding author: Mirko Barbuto (mirko.barbuto@unicusano.it).

¹ “Niccolò Cusano” University, Rome I-00166, Italy. ² Antenna Department, Elettronica S.p.A., Rome I-00131, Italy. ³ Department of Engineering, “Roma Tre” University, Rome I-00146, Italy.

The structure of this paper is as follows. In Section 2, we present the design of a low-profile antenna based on the use of two meandered monopoles with the same dimensions. However, due to its narrow bandwidth, this structure cannot be used to cover the entire frequency spectrum of Wi-Fi systems. Therefore, in Section 3, we slightly change the dimensions of one of the monopoles in order to obtain two resonant frequencies that are properly merged to cover the 2.4–2.485 GHz frequency band. Finally, in Section 4, we draw the conclusions.

2. ANTENNA DESIGN WITH EQUAL MEANDERED MONOPOLES

2.1. Antenna Structure

In order to show the benefit of using two slightly different monopoles in terms of the operating bandwidth, we first consider the design of an antenna with equal meandered monopoles. The structure, shown in Figs. 1–2, consists of a square ground plane and an FR-4 substrate ($\epsilon_r = 4.3$; $\tan \delta = 0.025$; thickness 1.6 mm) positioned orthogonal to it. Two orthogonal meandered monopoles connected to the ground are etched on one side of the dielectric substrate. On the other side, a bow-tie-like monopole connected to the inner conductor of a 50 Ω coaxial cable is placed.

By properly co-designing the dimensions of the parasitic monopoles and the length of the driven bow-tie, we can tune the resonant frequencies of the overall structure and obtain a good impedance matching. Moreover, thanks to the meandered structure, a low-profile antenna with overall dimensions of $21 \times 10.5 \times 1.6 \text{ mm}^3$ ($\lambda_0/6 \times \lambda_0/12 \times \lambda_0/75$, excluding the ground plane) has been obtained. Please note that the two meandered monopoles can be initially designed by using analytical formulas based on an equivalent circuit approach [20–22] or considering that the total length of each meandered monopole should be equal to $\lambda_{eff}/4$, where λ_{eff} is the operating wavelength taking into account the presence of a dielectric material [23].

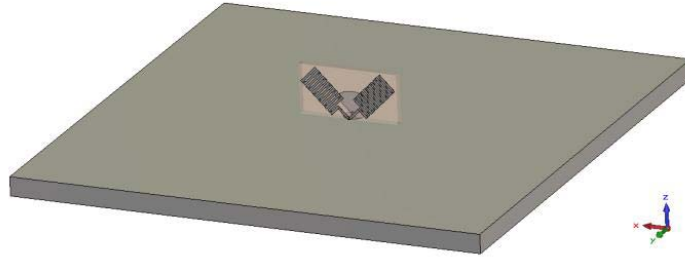


Figure 1. Perspective view of the proposed antenna. The ground side is 10 cm.

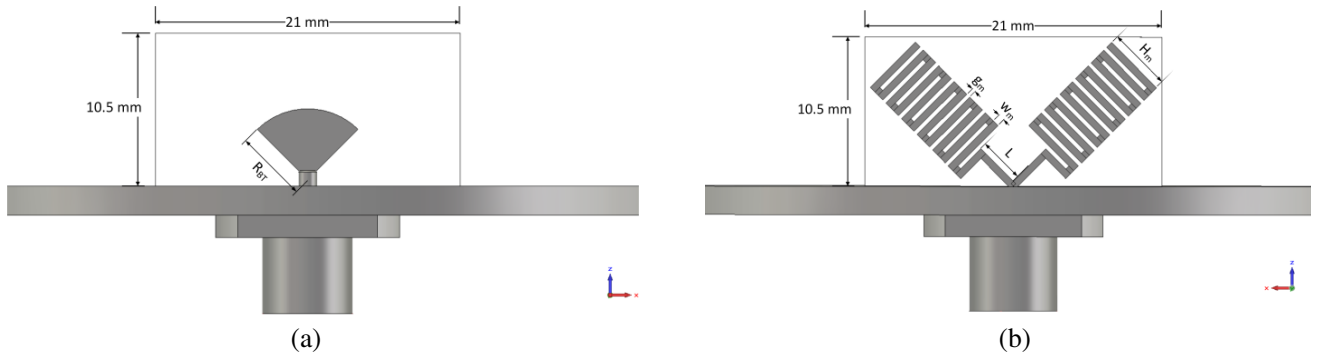


Figure 2. (a) Front view and (b) back view of the proposed antenna with equal meandered monopoles. Antenna dimensions are: $R_{BT} = 4.9 \text{ mm}$, $H_m = 4.5 \text{ mm}$, $g_m = 0.3 \text{ mm}$, $w_m = 0.48 \text{ mm}$, $L = 3 \text{ mm}$.

2.2. Simulation Results

The behavior of the structure presented in the previous subsection has been numerically evaluated by using the full-wave simulator CST Microwave Studio [24]. The reflection coefficient, reported in Fig. 3, shows good impedance matching around 2.4 GHz. However, due to the same length of the two monopoles, only one resonant frequency with a 2% –10 dB fractional bandwidth is obtained. Therefore, this antenna cannot cover the entire Wi-Fi band at 2.4 GHz. For this reason, in the next Section, we propose a modified structure with different monopole lengths leading to a larger impedance bandwidth.

For sake of completeness, in Fig. 4 we report also the radiation patterns at the resonant frequency of 2.425 GHz. The overall efficiency is around 65% within the whole impedance bandwidth. Finally, the surface currents on the two meandered monopoles at 2.425 GHz, shown in Fig. 5, have approximately the same intensity, confirming the single frequency resonant behavior.

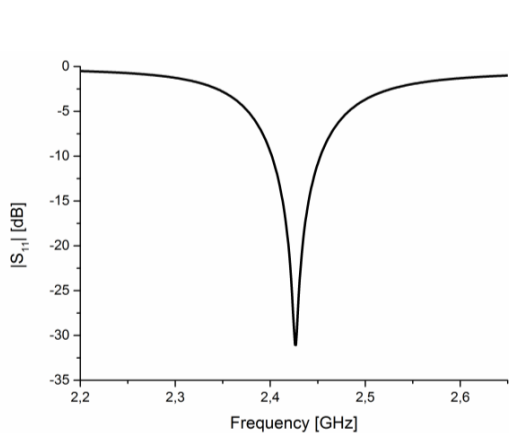


Figure 3. Reflection coefficient amplitude of the proposed antenna with equal meandered monopoles.

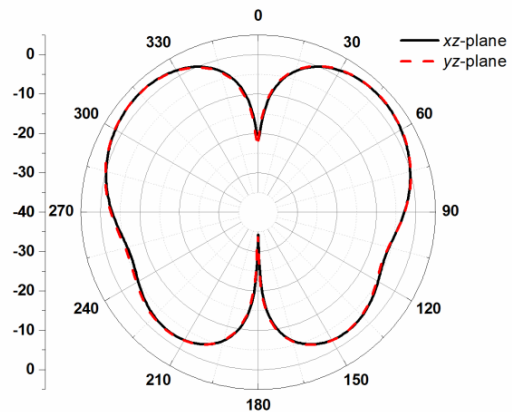


Figure 4. Realized gain patterns at the resonant frequency (2.425 GHz) of the antenna with equal meandered monopoles.

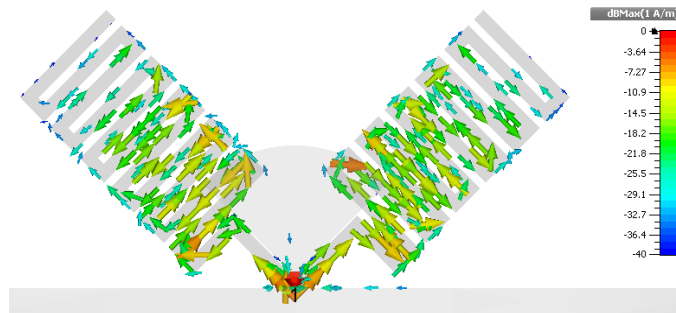


Figure 5. Surface currents on the two meandered monopoles at the resonant frequency of the overall structure (2.425 GHz).

3. ANTENNA DESIGN WITH SLIGHTLY DIFFERENT MEANDERED MONOPOLES

3.1. Antenna Structure

In Section 2, we have presented the design of a compact low-profile antenna by using two parasitic meandered monopoles and a driven bow-tie. As shown through proper full-wave simulations, this

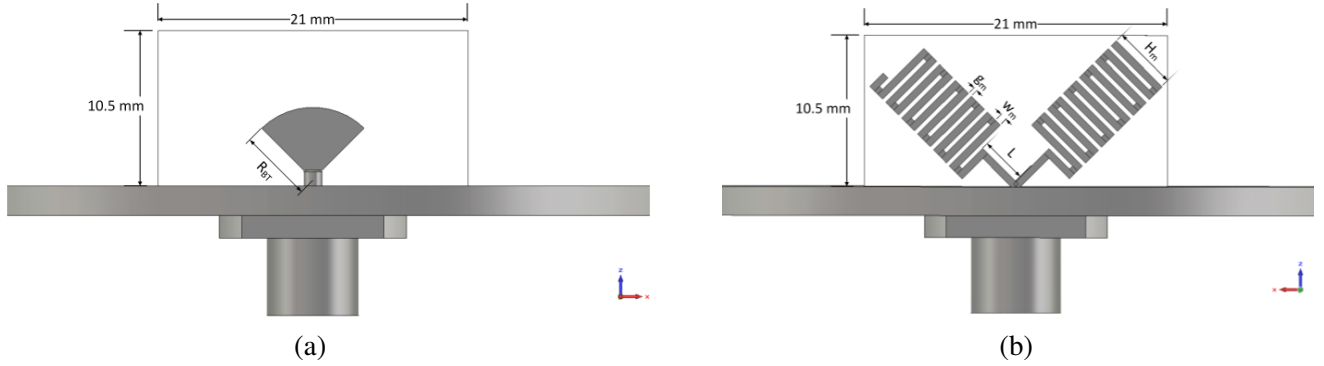


Figure 6. (a) Front view and (b) back view of the proposed antenna with slightly different meandered monopoles. Antenna dimensions are: $R_{BT} = 5$ mm, $H_m = 4.5$ mm, $g_m = 0.3$ mm, $w_m = 0.48$ mm, $L = 3$ mm.

antenna has a narrow operating bandwidth that does not allow Wi-Fi operation within the 2.4 GHz band. In order to broaden the operating bandwidth, we propose here to use two slightly different meandered monopoles with different but close resonant frequencies.

The resulting structure and the corresponding dimensions are shown in Fig. 6. In particular, the lengths of the two meandered monopoles differ for 5 mm, while all the other dimensions of the two monopoles are the same.

3.2. Simulation Results

The simulated reflection coefficient, obtained by using CST Microwave Studio, is shown in Fig. 7 and compared to the previous case. By properly co-designing the bow-tie and the meandered monopoles, a good impedance matching is obtained. Moreover, due to the different dimensions of the monopoles, two slightly different resonant frequencies are readily apparent. In this way, the -10 dB fractional bandwidth broadens from 2% to 3.5% and allows covering the entire 2.4–2.485 GHz band assigned to the Wi-Fi systems.

In particular, as it can be seen from Figs. 8 and 9, the shorter meandered monopole resonates at 2.416 GHz, while the longer one at 2.461 GHz. These frequencies correspond to the two negative peaks of the reflection coefficient.

Please note that, differently from the previous case, the overall efficiency is altered by the presence

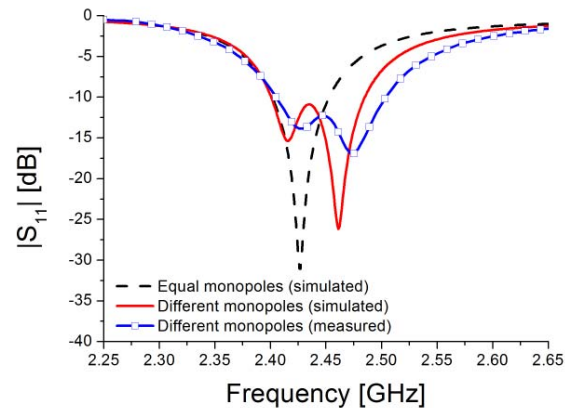


Figure 7. Reflection coefficient amplitude of the proposed antenna with slightly different monopoles (simulated and measured), compared to the one of the previous case.

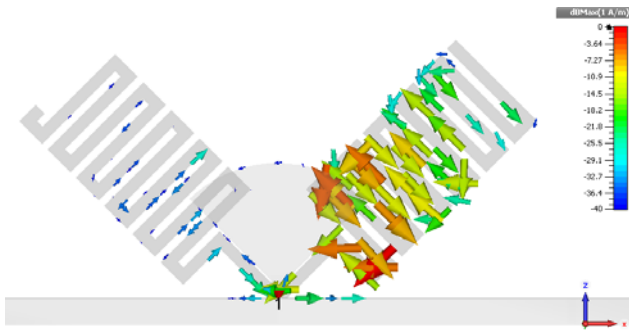


Figure 8. Surface currents on the two meandered monopoles at the lower resonant frequency of the overall structure shown in Fig. 6.

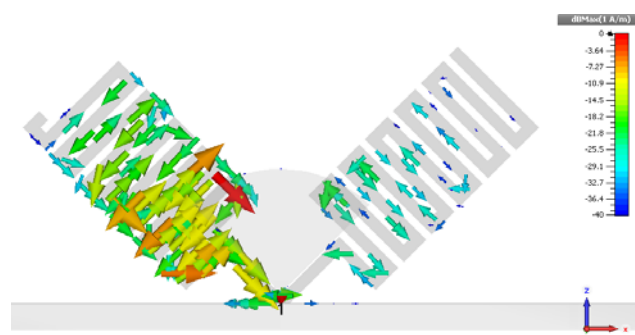


Figure 9. Surface currents on the two meandered monopoles at the higher resonant frequency of the overall structure shown in Fig. 6.

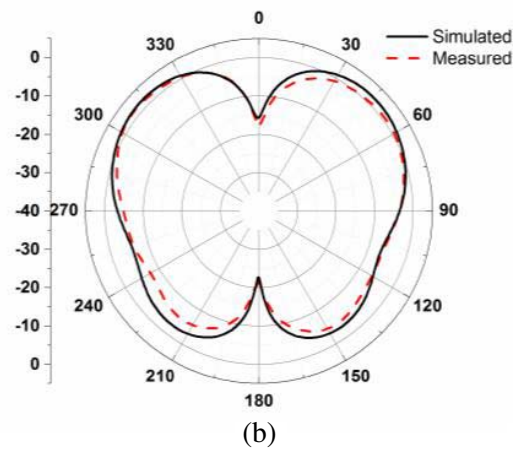
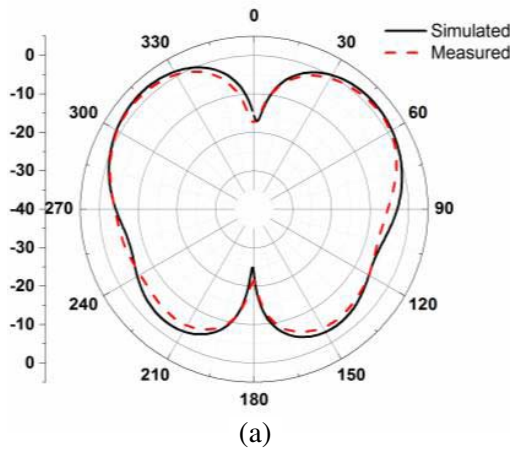


Figure 10. Realized gain patterns at the lower resonant frequency (2.416 GHz) of the antenna with slightly different monopoles for both (a) xz - and (b) yz -planes.

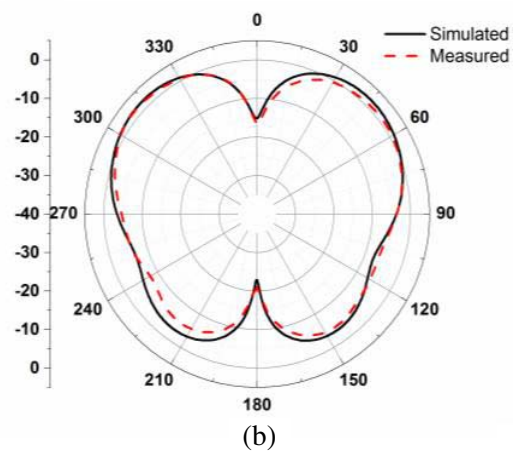
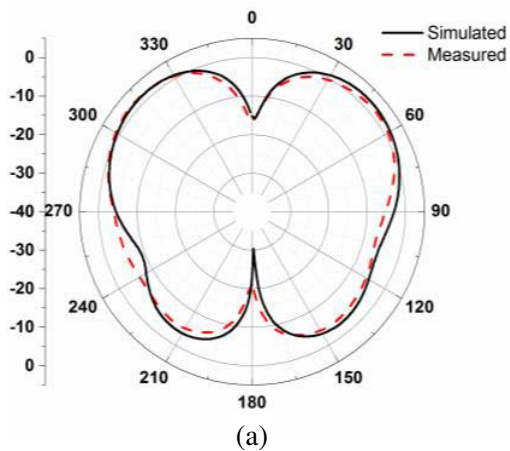


Figure 11. Realized gain patterns at the higher resonant frequency (2.461 GHz) of the antenna with slightly different monopoles for both (a) xz - and (b) yz -planes.

of the not-excited monopole. Despite this, an overall efficiency of around 50% is still obtained through full-wave numerical simulations. Finally, the radiation patterns at the two resonant frequencies are reported in Figs. 10–11.

4. FABRICATION AND MEASUREMENT

According to our design, a prototype has been realized to validate the proposed antenna with slightly different meandered monopoles. In particular, the two meandered monopoles and the driven bow-tie have been etched on the two faces of a 1.6 mm-thick FR-4 substrate, respectively, using the LPKF Protomat-S milling machine. Then, this block has been mounted on a 100×100 -mm² square ground plane by using hot melt glue and a thin foam layer. Finally, the inner conductor of a 50 Ω SMA connector has been soldered to the driven bow-tie through the ground plane, while the external conductor has been welded to the ground. The overall structure is shown in Fig. 12.

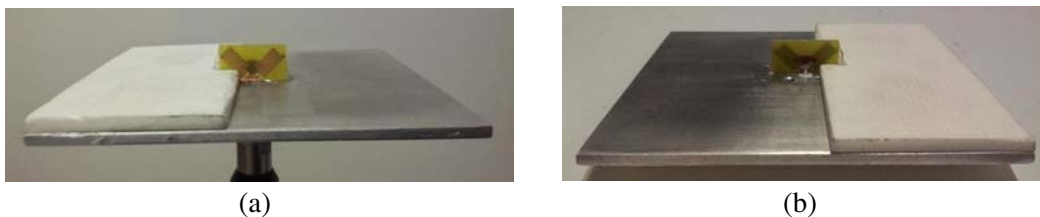


Figure 12. Photographs showing the (a) front view and (b) back view of the realized prototype.

The reflection coefficient magnitude at the input port, measured with a vector network analyzer Rodhe & Schwartz ZVB 4, is shown in Fig. 7, where it can be seen that -10 dB impedance matching is achieved over the bandwidth 2.4–2.51 GHz. The measured radiation patterns of the antenna for both xz - and yz -planes, obtained by using a near-field antenna measurement system, are shown in Figs. 10–11 for 2.416 and 2.461 GHz, respectively. The good agreement between simulated and measured performance validates the design.

5. CONCLUSIONS

In this work, we have first presented a low-profile antenna consisting of two orthogonal meandered monopoles that act as parasitic elements of a driven bow-tie. Then, we have shown that, by using two monopoles with slightly different dimensions, a broader impedance bandwidth can be obtained. Using this approach, we have presented a low-profile antenna operating in the 2.4 GHz Wi-Fi band with overall dimensions of $21 \times 10.5 \times 1.6$ mm³ ($\lambda_0/6 \times \lambda_0/12 \times \lambda_0/75$). Fabrication and test of a prototype confirm the effectiveness of the proposed design.

ACKNOWLEDGMENT

The authors would like to thank Elettronica S.p.A. for providing measurement instrumentation.

REFERENCES

1. Puente-Baliarda, C., J. Romeu, R. Pous, and A. Cardama, “On the behavior of the Sierpinski multiband fractal antenna,” *IEEE Trans. Antennas Propag.*, Vol. 46, 517–528, Apr. 1998.
2. Puente-Baliarda, C., J. Romeu, and A. Cardama, “The Koch monopole: A small fractal antenna,” *IEEE Trans. Antennas Propag.*, Vol. 48, 1773–1781, Nov. 2000.
3. Best, S. R., “On the performance properties of the Koch fractal and other bent wire monopoles,” *IEEE Trans. Antennas Propag.*, Vol. 51, 1292–1300, Jun. 2003.

4. Pan, S. C. and K. L. Wong, "Dual frequency triangular microstrip antenna with a shorting pin," *IEEE Trans. Antennas Propag.*, 1889–1891, Dec. 1997.
5. Barbuto, M., F. Bilotti, and A. Toscano, "Design of a multifunctional SRR-loaded printed monopole antenna," *Int. J. RF Microw. CAE*, Vol. 22, 552–557, 2012.
6. Hansen, R. C., "Fundamental limitations in antennas," *Proceedings of the IEEE*, Vol. 69, 170–182, Feb. 1981.
7. McLean, J. S., "A re-examination of the fundamental limits on the radiation Q of electrically small antennas," *IEEE Trans. Antennas Propag.*, Vol. 44, 672–676, May 1996.
8. Collin, R. and S. Rothschild, "Evaluation of antenna Q," *IEEE Trans. Antennas Propag.*, Vol. 12, 23–27, Jan. 1964.
9. Jin, P. and R. W. Ziolkowski, "Multiband extensions of the electrically small near field resonant parasitic Z antenna," *IEEE Trans. Antennas Propag.*, Vol. 4, 1016–1025, Aug. 2010.
10. Barbuto, M., F. Trotta, F. Bilotti, and A. Toscano, "A combined bandpass filter and polarization transformer for horn antennas," *IEEE Antennas Wireless Propag. Lett.*, Vol. 12, 1065–1068, 2013.
11. Barbuto, M., F. Bilotti, and A. Toscano, "Novel waveguide components based on complementary electrically small resonators," *Photonic Nanostruct.*, Vol. 12, 284–290, 2014.
12. Barbuto, M., F. Trotta, F. Bilotti, and A. Toscano, "Horn antennas with integrated notch filters," *IEEE Trans. Antennas Propag.*, Vol. 63, 781–785, 2015.
13. Zhu, J., M. A. Antoniades, and G. V. Eleftheriades, "A compact tri-band monopole antenna with single-cell metamaterial loading," *IEEE Trans. Antennas Propag.*, Vol. 58, 1031–1038, Apr. 2010.
14. Jin, P. and R. W. Ziolkowski, "Multi-frequency, linear and circular polarized, metamaterial-inspired, near-field resonant parasitic antennas," *IEEE Trans. Antennas Propag.*, Vol. 59, No. 5, 1446–1459, May 2011.
15. Jin, P., C. C. Lin, and R. W. Ziolkowski, "Multifunctional, electrically small, planar near-field resonant parasitic antennas," *IEEE Antennas Wireless Propag. Lett.*, Vol. 11, 200–204, 2012.
16. Barbuto, M., A. Monti, F. Bilotti, and A. Toscano, "Design of a non-foster actively loaded SRR and application in metamaterial-inspired components," *IEEE Trans. Antennas Propag.*, Vol. 61, No. 3, 1219–1227, Mar. 2013.
17. Erentok, A. and R. W. Ziolkowski, "Metamaterial-inspired efficient electrically small antenna," *IEEE Trans. Antennas Propag.*, Vol. 56, No. 3, 691–707, Mar. 2008.
18. Barbuto, M., F. Trotta, F. Bilotti, and A. Toscano, "Varying the operation bandwidth of metamaterial-inspired filtering modules for horn antennas," *Progress In Electromagnetics Research C*, Vol. 58, 61–68, 2015.
19. Du, G.-H., X. Tang, and F. Xiao, "Tri-band metamaterials-inspired monopole antenna with modified S-shaped resonator," *Progress In Electromagnetics Research Letters*, Vol. 23, 39–48, 2011.
20. Das, A., S. Dhar, and B. Gupta, "Lumped circuit model analysis of meander line antennas," *Proceedings of MMS 2011*, 21–24, 2011.
21. Olaode, O. O., W. D. Palmer, and W. T. Joines, "Characterization of meander dipole antennas with a geometry-based, frequency-independent lumped element model," *IEEE Antennas Wireless Propag. Lett.*, Vol. 11, 346–349, 2012.
22. Hosono, R., N. Guan, H. Tayama, and H. Furuya, "An equivalent circuit model for meander-line monopole antenna attached to metallic plate," *Proceedings of ISAP 2012*, 1421–1424, 2012.
23. Barbuto, M., A. Alù, F. Bilotti, A. Toscano, and L. Vegni, "Characteristic impedance of a microstrip line with a dielectric overlay," *COMPEL — The International Journal for Computation and Mathematics in Electrical and Electronic Engineering*, Vol. 32, No. 6, 1855–1867, 2013.
24. CST Studio Suite 2014, CST Computer Simulation Technology AG, Darmstadt, Germany [Online], available: <http://www.cst.com>.